J|A|C|S COMMUNICATIONS

Published on Web 10/15/2009

Self-Assembly and Traveling Wave Ion Mobility Mass Spectrometry Analysis of Hexacadmium Macrocycles

Yi-Tsu Chan,[†] Xiaopeng Li,[‡] Monica Soler,[†] Jin-Liang Wang,[†] Chrys Wesdemiotis,*[,†,‡] and George R. Newkome*[,†,‡]

Departments of Polymer Science and Chemistry, The University of Akron, Akron, Ohio 44325-3601

Received August 27, 2009; E-mail: wesdemiotis@uakron.edu; newkome@uakron.edu

The self-assembly of designed building blocks has been extensively applied in the construction of supramolecular species.[1] The reversibility of weak bonding plays an important role in production of thermodynamically favored structures. Lehn,[2] Stang,[3] Fujita,[4] Mirkin,[5] and others[6] have demonstrated the construction of highly ordered architectures via coordination interactions. We have also isolated hexameric metallomacrocycles formed by a variety of tpy-M(II)-tpy (where tpy = 2,2′:6′,2″-terpyridine, M = Ru, Fe, and Zn) bonds.[7] Since it is often difficult to obtain a single crystal of this type of metal complexes for X-ray crystallography, mass spectrometry analysis becomes an essential tool. Many organometallic assemblies have been detected and characterized by electrospray ionization (ESI) mass spectrometry under mild ionization conditions.[8] As a variety of ESI, cold-spray ionization (CSI) was developed to improve the signal intensities of labile species, especially those in which noncovalent interactions are prominent.[9] With its high resolving power, Fourier transform mass spectrometry (FTMS) allows one to investigate the isotope patterns in a broad distribution of different charge states;[8b,10] however, in all studies so far, the peaks from different charge states and shapes were superimposed. This problem can be resolved by traveling wave ion mobility mass spectrometry (TWIM-MS),[11] which enables two-dimensional gas-phase separation and complete deconvolution of the isotope patterns of ions with the same *m*/*z* value, thus substantially facilitating the structural analysis for self-assembled supramolecules. With TWIM-MS, ions with different charges and ions with cyclic and linear shapes are separated based on their drift time in the ion mobility device. The separated structures or charge states are subsequently characterized by their mass spectra and their fragmentation patterns in tandem mass spectra.

TWIM-MS is a variant of ion mobility mass spectrometry (IM-MS),[12] which within the past decade has developed into a particularly useful method for differentiating isobars, isomers, and conformers from biomolecules and biopolymers,[12] and more recently synthetic polymers, as well.[13] Herein, we report the preparation in high yield of hexagonal macrocycles and linear polymers with the labile tpy-Cd(II)-tpy (L-Cd^{2+}-L) connectivity[14] and the first characterization of such compounds by TWIM-MS.

Scheme 1 shows the three building blocks that were used to construct hexagonal macrocycles and linear polymers. Bisterpyridines **1** and **2** were synthesized according to our previous procedures.[7a,d] 2,3,5,6-Tetramethylterephthalaldehyde (Supporting Information) was ground with 5.5 equiv of 2-acetylpyridine via the mortar and pestle procedure[15] under basic conditions, and the mixture was then refluxed with NH_4OH in EtOH to give the desired rigid monomer **3** (30%). The structure **3** was established (^{1}H NMR) by the presence of peaks at 8.37 (3′,5′-tpy*H*s), 7.91 (4,4″-tpy*H*s), 7.36 (5,5″-tpy*H*s), and 2.04 ppm (CH_3).

Scheme 1. Self-Assembly of Hexameric Metallomacrocycles **4** and **5** and Linear Polymer **6**[a]

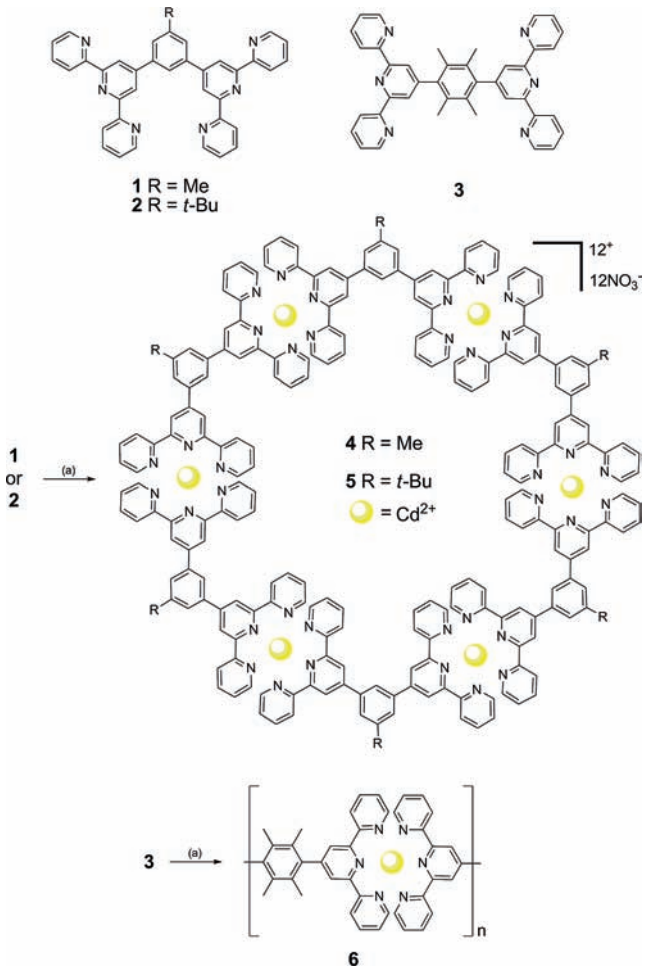

[a] Reagents and conditions: $Cd(NO_3)_2 \cdot 4H_2O$, $CHCl_3$/MeOH (3:2), 25 °C, 1 h.

Reactions of **1** and **2** with 1 equiv of $Cd(NO_3)_2 \cdot 4H_2O$ in $CHCl_3$/MeOH (3:2) afforded the hexacadmium macrocycles **4** and **5** in quantitative yields. Their ^{1}H NMR and ^{13}C NMR spectra agreed with the structures given in Scheme 1 (see Supporting Information and Figure S1). The hexameric composition of **4** was further confirmed by ESI-MS peaks at *m*/*z* 2311.1, 1520.5, 1124.3, 888.0, and 729.1, corresponding to +2 to +6 charge states, respectively. Similarly, the ESI mass spectrum of **5** confirmed the presence of a hexameric complex with signals at *m*/*z* 2437.9, 1604.6, 1187.9, 937.9, and 771.3 for the species in charge states +2 to +6, respectively.

[†] Department of Polymer Science.
[‡] Department of Chemistry.

10.1021/ja907262c CCC: $40.75

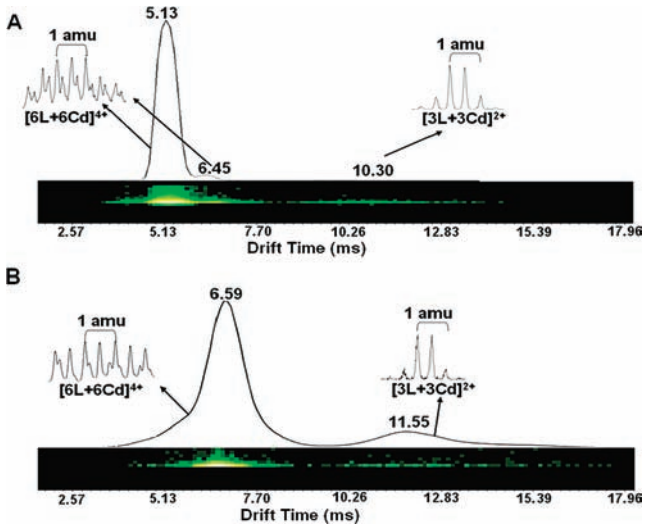

Figure 1. Two-dimensional ESI-TWIM-MS plot for *m*/*z* 1188. (A) Complex **5** analyzed on the Waters Synapt quadrupole/time-of-flight (Q/ToF) mass spectrometer at a traveling wave height of 9.3 V and velocity of 380 m/s. Ion mobility separation gave signals at 10.30, 6.45, and 5.13 ms, corresponding to linear $[3L+3Cd]^{2+}$, linear $[6L+6Cd]^{4+}$, and cyclic $[6L+6Cd]^{4+}$, respectively. The observed isotope patterns (shown) match closely those calculated for the mentioned compositions. (B) Complex **6** analyzed under the same conditions. Ion mobility separation showed signals at 11.55 and 6.59 ms, corresponding to linear $[3L+3Cd]^{2+}$ and linear $[6L+6Cd]^{4+}$, respectively. As expected, no cyclic $[6L+6Cd]^{4+}$ was observed from complex **6**.

A stirred solution of monomer **3** and $Cd(NO_3)_2 \cdot 4H_2O$ in a 1:1 ratio at 25 °C gave the linear polymer **6**. The ^1H NMR spectrum of **6** exhibited unique signals, all of which were much broader than those in the spectra of macrocycles **4** and **5**, consistent with a polymeric linear, not macrocyclic, structure.

The corresponding ESI spectra mostly consist of a series of differently charged complexes, including the hexameric Cd(II) macrocycle and linear fragments. Full spectra of complex **4**, **5**, and **6** are given in Figures S2, S3, and S4, respectively; the *m*/*z* values of the observed peaks agree with the assemblies carrying a varying number of charges, as summarized in Tables S1 and S2. For example, *m*/*z* 1188 corresponds to linear $[3L+3Cd]^{2+}$ (this complex also contains four NO_3^- counterions which are omitted from the acronym for brevity), linear $[6L+6Cd]^{4+}$, or cyclic $[6L+6Cd]^{4+}$. Note that combinations equal to or larger than $[9L+9Cd]^{6+}$ have not been considered, because the formation of such large complexes is entropically disfavored.

The ions at *m*/*z* 1188 from **5** were selected for ion mobility separation due to the low number of L/Cd^{2+} combinations possible at this mass-to-charge ratio (Figure S3 and Table S2). Three species are detected after ion mobility separation (Figure 1A). Analysis of the corresponding isotope patterns reveals the presence of two charge states at *m*/*z* 1188, having spacings of $\Delta m = 0.5$ and 0.25 amu, respectively. The weak signal with the longer drift time, 10.30 ms, has an isotope spacing of $\Delta m = 0.5$ amu and corresponds to $[3L+3Cd]^{2+}$. The signals at shorter drift times, 5.13 and 6.45 ms, have an isotope spacing of $\Delta m = 0.25$ amu and correspond to $[6L+6Cd]^{4+}$. The two $[6L+6Cd]^{4+}$ ions should originate from cyclic and linear isomers. The question now is how to assign the proper structures to these two species. Inside the gas-filled ion mobility chamber, ions are separated not only on the basis of their *m*/*z* ratios but also according to their shapes. Compact molecular ions drift faster, while more extended structures drift more slowly during the separation.[12] Hence, cyclic $[6L+6Cd]^{4+}$ is assumed to have the 5.13-ms drift time, and linear $[6L+6Cd]^{4+}$ is assumed to have the 6.45-ms drift time.

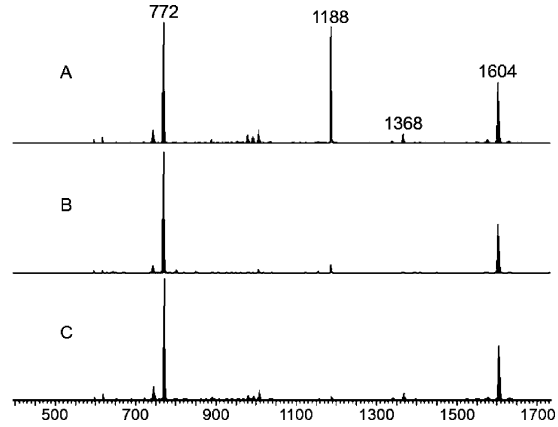

Figure 2. Tandem mass spectra of *m*/*z* 1188. (A,B) Precursors of *m*/*z* 1188 from complex **5** (A) remained in high abundance at a trap collision energy of 16.0 eV but (B) dissociated almost completely at a trap collision energy of 22.5 eV. (C) Precursors of *m*/*z* 1188 from complex **6** dissociated almost completely already at the collision energy of 16.0 eV.

To validate our assumption, monomer **3**, which has an 180°-angle geometry and is an isomer of ligand **2**, was utilized to synthesize complex **6** for comparison with complex **5**. Ligand **3** is constrained to form linear assemblies. In Figure 1B, signals for two species from **6** are observed, corresponding to linear $[3L+3Cd]^{2+}$ (trace), and linear $[6L+6Cd]^{4+}$. The isotope patterns are identical to those observed from **5**. The drift time of linear $[3L+3Cd]^{2+}$ from **6**, 11.55 ms, is longer than that of $[3L+3Cd]^{2+}$ from **5**, which was synthesized using the 120°-angle building block **2**. $[3L+3Cd]^{2+}$ from **6** contains 180°-angle blocks instead and, thus, is longer than $[3L+3Cd]^{2+}$ from **5**, explaining its longer drift time. Similarly, linear $[6L+6Cd]^{4+}$ from **6** is observed at a 6.59-ms drift time, which is slightly longer than the 6.45 ms for linear $[6L+6Cd]^{4+}$ from **5**. Most importantly, no signals are detected around 5.13 ms for **6**. This confirms that the signal at 5.13 ms in Figure 1A arises from cyclic $[6L+6Cd]^{4+}$, while that at 6.45 ms is a linear $[6L+6Cd]^{4+}$ isomer.

The tandem mass spectra of *m*/*z* 1188 provide further evidence for the existence of linear and cyclic $[6L+6Cd]^{4+}$ isomers in **5**. In the tandem mode of the Synapt mass spectrometer, *m*/*z* 1188 was selected by the quadrupole and fragmented in the trap cell at different collision energies. The *m*/*z* 1188 ion from **6** almost disappears at 16.0 eV (Figure 2C). In contrast, *m*/*z* 1188 from **5** still remains largely intact at 16.0 eV (Figure 2A). Only when the trap bias is increased to 22.5 eV, *m*/*z* 1188 from **5** almost disappears by fragmentation (Figure 2B). This difference corroborates the presence of macrocyclic isomers in $[6L+6Cd]^{4+}$ from **5**; these are expected to be more stable than isomeric linear structures because cyclics require cleavage of more bonds for fragmentation. Thus, the tandem mass spectra confirm the existence of intact cyclic $[6L+6Cd]^{4+}$ ions in complex **5**.

Ion mobility analysis was also performed on the ions at *m*/*z* 1604, which are the highest *m*/*z* products observed with sizable abundance (Figure 3). From complex **5**, four species are clearly separated by their ion mobilities. Analysis of the corresponding isotope patterns reveals the presence of four charge states in *m*/*z* 1604 with isotope spacings of $\Delta m = 1.0$, 0.50, 0.33, and 0.25 amu. From high to low charge state, the signals observed are $[8L+8Cd]^{4+}$ appearing at 2.71 ms; $[6L+6Cd]^{3+}$ appearing at 3.61 ms; $[4L+4Cd]^{2+}$ appearing at 4.78 ms; and $[2L+2Cd]^{1+}$ appearing at 10.11 ms (Figure 3A). The ions of $[4L+4Cd]^{2+}$ and $[2L+2Cd]^{1+}$ are assigned to linear fragments produced during the ionization process. Due to the high abundance of $[4L+4Cd]^{2+}$, some $[8L+8Cd]^{4+}$ ions are also detected in complex **5**. Because of the 120°-angle in the

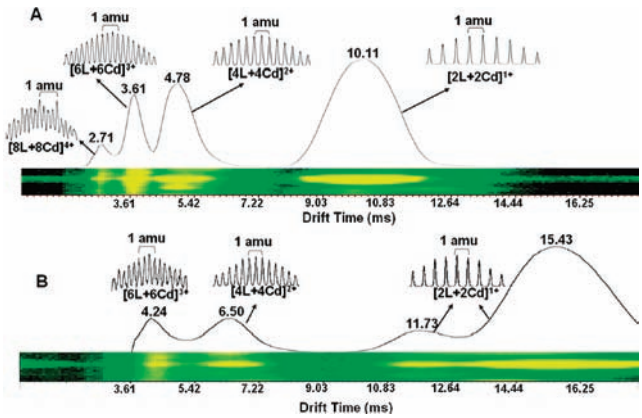

Figure 3. Two-dimensional ESI-TWIM-MS plot for *m/z* 1604. (A) Complex **5** analyzed at a traveling wave height of 10.5 V and velocity of 380 m/s. Ion mobility separation gave signals at 10.11, 4.78, 3.61, and 2.71 ms, corresponding to linear $[2L+2Cd]^{1+}$, linear $[4L+4Cd]^{2+}$, cyclic $[6L+6Cd]^{3+}$, and linear $[8L+8Cd]^{4+}$, respectively. The observed isotope patterns (shown) match closely those calculated for the given compositions. (B) Complex **6** analyzed under the same conditions. Ion mobility separation showed signals at 15.43, 11.73, 6.50, and 4.24 ms, corresponding to linear $[2L+2Cd]^{1+}$, $[2L+2Cd]^{1+}$, $[4L+4Cd]^{2+}$, and $[6L+6Cd]^{3+}$, respectively.

building blocks, there is a general trend for such species to form hexameric macrocycles, which are geometrically most easily accessible. Thus, the $[8L+8Cd]^{4+}$ ions most likely have linear shapes. For the $[6L+6Cd]^{3+}$ ions, both linear and cyclic conformers can exist; however, only one shape is observed or the two shapes were not resolved. As discussed above, the charge state 4+, i.e. $[6L+6Cd]^{4+}$ at *m/z* 1188, contains much more cyclic than linear isomers. Consequently, cyclic $[6L+6Cd]^{3+}$ should be the major species of the 3+ charge state of *m/z* 1604 as well. The drift time of linear $[6L+6Cd]^{3+}$ ions might be very close to that of the $[4L+4Cd]^{2+}$ fragments. Any minor amount of linear $[6L+6Cd]^{3+}$ would then drift out between the cyclic $[6L+6Cd]^{3+}$ and linear $[4L+4Cd]^{2+}$ species, i.e. within the 3.61−4.78 ms time window.

Also *m/z* 1604 from **6** was analyzed by TWIM-MS (Figure 3B). Ion mobility separation showed signals at 4.24, 6.50, 11.73, and 15.43 ms corresponding to linear $[6L+6Cd]^{3+}$, $[4L+4Cd]^{2+}$, $[2L+2Cd]^{1+}$, and $[2L+2Cd]^{1+}$, respectively. The isotope patterns closely matched those calculated for each of these charge states. This time, no signal for $[8L+8Cd]^{4+}$ was observed in the spectrum. The reason could be that long strains of linear complexes decompose readily upon ionization and ion mobility separation. Because of the 180°-angle of building blocks in **6**, its ions show longer drift times than the corresponding ions from **5**, as also observed for *m/z* 1188. It is noteworthy that no signal is observed around 3.61 ms confirming the cyclic shape for $[6L+6Cd]^{3+}$ from **5**. Based on this comparison, linear $[6L+6Cd]^{3+}$ ions with 120°-angle monomers should drift out between cyclic $[6L+6Cd]^{3+}$ with 120°-angle building blocks and linear $[6L+6Cd]^{3+}$ with 180°-angle building blocks, viz. between 3.61 and 4.24 ms. For the linear $[2L+2Cd]^{1+}$ fragment from **6**, two isomers were observed; their structures are currently under investigation.

In conclusion, we have successfully synthesized hexagonal metallomacrocycles and linear polymers by using the labile tpy-Cd(II)-tpy connectivity and showed that ion mobility separation enhances the resolving power of mass spectrometry by adding shape-dependent dispersion. This provides the possibility to identify isomeric structures in supramolecular assemblies. Further, TWIM-MS completely deconvolutes the isotope patterns of different charge states and avoids the isomer superposition prevalent in regular ESI-MS or FTMS. Tandem mass spectrometry experiments confirmed the structural information obtained from ion mobility separation. The recently introduced second generation Synapt G2 platform provides enhanced ion mobility and mass resolution. Combination of ESI with ion mobility separation and tandem MS fragmentation are therefore expected to have a significant impact on supramolecular characterizations.

Acknowledgment. We thank the NSF for generous financial support (Grants CHE-0517909 and 0833087 to C.W., DMR-0705015 to G.R.N., and DMR-0821313 for the purchase of the TWIM-MS instrument).

Supporting Information Available: Synthetic procedures, NMR data, complete ESI mass spectra, and tables of the possible charge states and mass-to-charge ratios.This material is available free of charge via the Internet at http://pubs.acs.org.

References

(1) *Supramolecular Chemistry: Concepts and Perspectives*; Lehn, J.-M.; VCH: Weinheim, 1995.
(2) (a) Lehn, J. M. *Chem.—Eur. J.* **1999**, *5*, 2455. (b) Lehn, J. M. *Science* **2002**, *295*, 2400. (c) Ruben, M.; Rojo, J.; Romero-Salguero, F. J.; Uppadine, L. H.; Lehn, J. M. *Angew. Chem., Int. Ed.* **2004**, *43*, 3644.
(3) (a) Northrop, B. H.; Yang, H. B.; Stang, P. J. *Chem. Commun.* **2008**, 5896. (b) Li, S. S.; Northrop, B. H.; Yuan, Q. H.; Wan, L. J.; Stang, P. J. *Acc. Chem. Res.* **2009**, *42*, 249. (c) Northrop, B. H.; Zheng, Y. R.; Chi, K. W.; Stang, P. J. *Acc. Chem. Res.* **2009**,in press (DOI: 10.1021/ar900077c).
(4) (a) Fujita, M.; Tominaga, M.; Hori, A.; Therrien, B. *Acc. Chem. Res.* **2005**, *38*, 369. (b) Yoshizawa, M.; Klosterman, J. K.; Fujita, M. *Angew. Chem., Int. Ed.* **2009**, *48*, 3418.
(5) (a) Holliday, B. J.; Mirkin, C. A. *Angew. Chem., Int. Ed.* **2001**, *40*, 2022. (b) Gianneschi, N. C.; Masar, M. S.; Mirkin, C. A. *Acc. Chem. Res.* **2005**, *38*, 825. (c) Oliveri, C. G.; Ulmann, P. A.; Wiester, M. J.; Mirkin, C. A. *Acc. Chem. Res.* **2008**, *41*, 1618.
(6) (a) Lee, S. J.; Lin, W. *Acc. Chem. Res.* **2008**, *41*, 521. (b) Kumar, A.; Sun, S. S.; Lees, A. J. *Coord. Chem. Rev.* **2008**, *252*, 922. (c) Constable, E. C. *Coord. Chem. Rev.* **2008**, *252*, 842.
(7) (a) Newkome, G. R.; Cho, T. J.; Moorefield, C. N.; Baker, G. R.; Saunders, M. J.; Cush, R.; Russo, P. S. *Angew. Chem., Int. Ed.* **1999**, *38*, 3717. (b) Newkome, G. R.; Cho, T. J.; Moorefield, C. N.; Cush, R.; Russo, P. S.; Godinez, L. A.; Saunders, M. J.; Mohapatra, P. *Chem.—Eur. J.* **2002**, *8*, 2946. (c) Newkome, G. R.; Cho, T. J.; Moorefield, C. N.; Mohapatra, P. P.; Godinez, L. A. *Chem.—Eur. J.* **2004**, *10*, 1493. (d) Hwang, S.-H.; Moorefield, C. N.; Wang, P.; Kim, J.-Y.; Lee, S.-W.; Newkome, G. R. *Inorg. Chim. Acta* **2007**, *360*, 1780.
(8) (a) Wang, P.; Newkome, G. R.; Wesdemiotis, C. *Int. J. Mass Spectrom.* **2006**, *255−256*, 86. (b) Engeser, M.; Rang, A.; Ferrer, M.; Gutierrez, A.; Baytekin, H. T.; Schalley, C. A. *Int. J. Mass Spectrom.* **2006**, *255−256*, 185. (c) Ghosh, K.; Hu, J.; White, H. S.; Stang, P. J. *J. Am. Chem. Soc.* **2009**, *131*, 6695.
(9) (a) Sakamoto, S.; Fujita, M.; Kim, K.; Yamaguchi, K. *Tetrahedron* **2000**, *56*, 955. (b) Yamaguchi, K. *J. Mass Spectrom.* **2003**, *38*, 473.
(10) Schalley, C. A.; Muller, T.; Linnartz, P.; Witt, M.; Schafer, M.; Lutzen, A. *Chem.—Eur. J.* **2002**, *8*, 3538.
(11) Pringle, S. D.; Giles, K.; Wildgoose, J. L.; Williams, J. P.; Slade, S. E.; Thalassinos, K.; Bateman, R. H.; Bowers, M. T.; Scrivens, J. H. *Int. J. Mass Spectrom.* **2007**, *261*, 1.
(12) (a) Von Helden, G.; Hsu, M.-T.; Kemper, P. R.; Bowers, M. T. *J. Chem. Phys.* **1991**, *95*, 3835. (b) Bowers, M. T.; Kemper, P. R.; von Helden, G.; van Koppen, P. A. M. *Science* **1993**, *260*, 1446. (c) Clemmer, D. E.; Jarrold, M. F. *J. Mass Spectrom.* **1997**, *32*, 577. (d) Hoaglund-Hyzer, C. S.; Counterman, A. E.; Clemmer, D. E. *Chem. Rev.* **1999**, *99*, 3037. (e) Verbeck, G. F.; Ruotolo, B. T.; Sawyer, H. A.; Gillig, K. J.; Russel, D. H. *J. Biomol. Tech.* **2002**, *13*, 56. (f) Valentine, S. J.; Plasencia, M. D.; Liu, X.; Krishnan, M.; Naylor, S.; Udseth, H. R.; Smith, R. D.; Clemmer, D. E. *J. Proteom. Res.* **2006**, *5*, 2977. (g) Fenn, L. S.; McLean, J. A. *Anal. Bioanal. Chem.* **2008**, *391*, 1618. (h) Ruotolo, B. T.; Benesch, J. L. P.; Sandercock, A. M.; Hyung, S.-J.; Robinson, C. V. *Nat. Protoc.* **2008**, *3*, 1139. (i) Kanu, A. B.; Dwivedi, P.; Tam, M.; Matz, L.; Hill, H. H. *J. Mass Spectrom.* **2008**, *43*, 1. (j) Bohrer, B. C.; Merenbloom, S. I.; Koeniger, S. L.; Hilderbrand, A. E.; Clemmer, D. E. *Annu. Rev. Anal. Chem.* **2008**, *1*, 293.
(13) (a) Trimpin, S.; Plasencia, D. I.; Clemmer, D. E. *Anal. Chem.* **2007**, *79*, 7965. (b) Anderson, S. E.; Bodzin, D. J.; Haddad, T. S.; Boatz, J. A.; Mabry, J. M.; Mitchell, C.; Bowers, M. T. *Chem. Mater.* **2008**, *20*, 4299. (c) Trimpin, S.; Clemmer, D. E. *Anal. Chem.* **2008**, *80*, 9073. (d) Hilton, G. R.; Jackson, A. T.; Thalassinos, K.; Scrivens, J. H. *Anal. Chem.* **2008**, *80*, 9720. (e) Gies, A. P.; Kliman, M.; McLean, J. A. *Macromolecules* **2008**, *41*, 8299.
(14) ; Schubert, U. S.; Hofmeier, H.; Newkome, G. R. *Modern Terpyridine Chemistry*; Wiley-VCH: Weinheim, 2006.
(15) Cave, G. W. V.; Raston, C. L. *J. Chem. Soc., Perkin Trans. 1* **2001**, 3258.

JA907262C